Observation of Twin Boundary Migration in Copper During Deformation

[1]D.P. Field, [1]B.W. True, [2]T.M. Lillo, [3]J.E. Flinn

[1]School of Mechanical and Materials Engineering, Washington Sta an, WA 99164-2920

[2]Idaho National Engineering and Environmental Laboratory, P. Falls, ID 83415

[3]University of Idaho—Idaho 83402

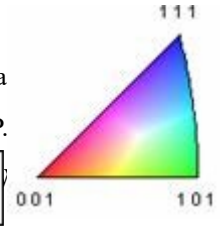

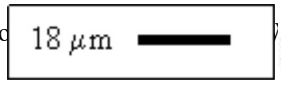

Abstract

A previous investigation produced evidence that twin boundaries in annealed copper were a significant source of dislocations during the initial stages of plastic flow. The character of the dislocation source was unknown, but it was hypothesized that twin boundaries could be non-regenerative dislocation sources that would cause migration of the boundary during plastic deformation. Channel die deformation and intermittent orientation imaging were performed on split specimens of pure copper in an attempt to observe twin boundary migration. Approximately 15 percent of the twin boundaries were observed to migrate beyond that expected from the imposed strain. The data support the hypothesis that twin boundaries can serve as dislocation sources.

Introduction

In an earlier study, the authors reported observations on the influence of grain size on the flow stress behavior of polycrystalline copper [1]. The results of the study are summarized as follows: (1) the grain size including annealing twins only affected the onset of plastic flow showing no influence on strain hardening; (2) the flow stress dependence on grain size was associated with a reciprocal boundary (twin and grain) and not on an inverse square root dependence; (3) TEM images after small amounts of plastic deformation showed dislocation debris including loops along twin boundaries with few dislocations evident on random boundaries; and (4) orientation imaging showed unmistakably that the overall fraction of S3 boundaries were reduced during deformation. The strengthening from grain size, in particular the area of annealing twin boundary per unit volume, is associated with the activation of dislocation sources at the initial stages of plastic deformation. Since the grain size had no influence on the subsequent strain hardening of copper, it is evident that dislocation-dislocation interactions control hardening behavior. Dislocation interactions with grain and twin boundaries do not contribute significantly to strain hardening at larger strains where a refined dislocation network controls mechanical response of the metal.

The question that has not been significantly resolved is the character of the dislocation sources during the initial stages of plastic deformation. Our prior evidence [1] supports the interpretation that the annealing twin boundaries can be significant sources for dislocations. Other investigators have reached similar conclusions [2-5].

The experiments described in this present study on polycrystalline copper are designed to observe twin boundaries at incremental stages of deformation with the intent to determine whether the imposed strain causes the boundaries to migrate or somehow "unravel." Observation of the movement of an apparent coherent twin boundary would confirm that they are serving as non-regenerative dislocation sources (as opposed to the more common Frank-Read source that is regenerative in nature). We also expect that lattice curvature behind the migrating twin boundary to be significant. Measurement and quantification of these phenomena are the objective of this paper.

Experimental Procedure

The material used in the experiments was electronic grade copper (oxygen-free, high-conductivity – OFHC) that had been passed through an equal channel angular extrusion die using 4 passes of the B route [6-8]. The copper billet was subsequently annealed at 300ºC for 1 hour in Argon resulting in an average grain size of about 10 microns, excluding twins as grains. (When twins are included in the distribution the average grain diameter is about 4 microns.) The material was sectioned into pieces 4 x 4 x 22 mm^3 in dimension using a low speed diamond saw. The samples were ground and polished for orientation imaging analysis. Small black marks were made on the polished specimen surface for use as fiducial indicators so the same region could be analyzed after successive deformations. A separate slice of the same material was prepared to have a relatively large grain size (2 mm thick with an average grain size of 1 mm). This slice was polished and placed against the polished surface of the specimen of interest. The large grained specimen protected the surface on the specimen of interest from high shear strain at the specimen/die interface, as shown in Figure 1.

After initial microstructural characterization by orientation imaging, the two specimens were wrapped together with Teflon sheet to minimize friction between the die and the sample surface. The samples were placed into a channel die to enforce plane strain deformation conditions. The channel die consists of an open channel with a fixed floor and two parallel walls at fixed locations. Deformation occurs by displacement of the ram, which compresses the material and causes it to flow in positive and negative directions along the unconstrained axis. The large grained slice provided protection from severe shear deformation on the observation surface and also created a pseudo-internal observation plane that would simulate bulk behavior rather than surface phenomena [cf. 9]. Since the mating slice had such a large grain size compared with the specimen of interest, the probability was low that a grain boundary would cross the analysis region in the sample of interest during deformation. Therefore, it was assumed that all grains observed in the analysis were deformed against a single crystallite from the mating Cu piece and that the observed behavior was not merely an artifact of different boundary conditions imposed during deformation.

After deformation the samples were again analyzed by orientation imaging, and the process was repeated in steps of 5% height reduction up to 15% deformation. The samples were not polished between deformations so the same grains could be analyzed after each successive height reduction. The procedure was carried out

such that a relatively large analysis region was characterized after each strain increment with smaller step size orientation imaging scans made over regions of interest identified after each deformation. Figure 2 contains an orientation image of a portion of the typical analysis region from one of the specimens before deformation. The scans covered a region of approximately 90 x 180 μm^2 using a step size between neighboring measurement positions of 0.3 μm. Grains are colored according to the orientation color key given in Figure 2 that identifies the orientation of the crystallographic direction normal to the plane of the specimen surface. Two such regions from the mid-surface section of each specimen were repeatedly interrogated, and two identical specimens were deformed in the investigation. The black regions in each image indicate points that were not properly indexed during orientation imaging. The large black area on the top and near the right side shown in Figure 2 is one of the fiducial marks made on the specimen to identify the scan region. (These were made by surface marks that did not allow EBSD analysis, and hence are seen as non-indexed regions.)

Results and Discussion

Careful analysis of the twin boundaries at 0, 5, 10 and 15 percent reduction were made on the larger regions characterized. Generally it was observed that the twin boundaries did not appreciably migrate during deformation. Out of approximately 2500 twin boundaries individually observed and analyzed in this study, about 350 or 15% of the coherent and incoherent twin boundaries demonstrated significant boundary movement above that expected from specimen elongation alone. This observation in itself is not surprising since Taylor's assumption of uniform deformation in every grain is long known to be invalid in that it violates stress continuity across grain boundaries in polycrystalline materials. It is expected, however, that grains of high Taylor factor, *M*, will resist deformation in comparison to neighboring grains of relatively low *M*. To ensure that the apparent migration of the twin boundaries was not merely a consequence of "soft" grains deforming more than "hard" grains, Taylor factors were calculated for 100 pairs of twin and parent grains that appeared to migrate. If the observed migration of the boundary could be attributed to Taylor factor difference, it might be expected that the grain with the lower *M* would deform more than that with the higher *M*, making it appear that the boundary has migrated into the grain with the higher *M*. The range of Taylor factors calculated for all grains was 2.1 to 4.9. In 53 out of 100 pairs of grains analyzed (twins and parents), the Taylor factor was higher in the crystallite into which the boundary appeared to migrate. Figure 3 contains a chart showing the results of this analysis. Taylor factors are plotted for both the enlarging and the shrinking grain as a function of the fraction of deformation in the shrinking grain (after 10% compression in the channel die). A deformation fraction of 1.0 indicates that the grain has completely disappeared. The observation plane was normal to the axis of compression and if uniform deformation were to occur in each grain, the grains would extend 10 % along the extension direction, or they would not change dimension in the constrained direction. Only those grains were included in the analysis for which at least a 25% decrease in dimension in any direction was noted. The *M* data are widely scattered over the entire range of possible deformations. This apparent indifference to Taylor factor indicates that microstructural features other than lattice orientation are responsible for much of the observed boundary migration. Figure 4 shows orientation

images from a region of material before deformation and after 10% deformation. Two distinct twin grains are indicated that show the observed migration behavior. The twin grain on the left side of the image has a much lower Taylor factor than the parent grain, while the twin grain in the image center has a much higher Taylor factor than its parent. In each case, the twin grain shrinks in size along the vertical axis on the page, which is the extension axis of the channel die deformation.

In general, the fraction of twin boundaries decreased with increasing strain, as observed in the previous investigation [1]. Table 1 contains the overall fraction of twin boundaries observed in each specimen as determined by a tolerance angle of 2º to the exact relationship (60º about a <111> axis). Additionally, the lattice near the twin boundaries had rotated sufficiently during deformation that the misorientation relationship of S3 grain boundaries was lost or had rotated significantly from the ideal relationship. In a few isolated instances, a small twin boundary was observed to disappear completely with one side of the twin boundary migrating over to the mating boundary and annihilating the interface.

As an example case, Figure 5 contains orientation images after successive deformation steps up to 15% reduction on one such region. The image in Figure 5.a shows a pair of twin grains in the center of a parent grain in the undeformed state. Figures 5.b, 5.c, and 5.d show the same region in the specimen after 5, 10, and 15 percent height reduction. Figure 5.b shows that at 5% deformation, the lower twin in the image diminishes in size while the top twin appears to enlarge. In Figures 5.c and 5.d the lone remaining twin grain is seen at about the top-middle of the image. The area surrounding the twin, which has disappeared, is highly strained and can be seen in the colored image as the white area surrounding the twin (teal). The white area comes from lattice curvature resulting from extra half planes of atoms generated from the migrating twin boundary of the disappearing twin during deformation. The orientations of the parent and twin grains of the crystallites of interest are given together in the pole figure shown in Figure 6. These are the orientations measured before deformation. It is apparent that the common {111} plane, which is the coherent twin interface, is tilted only about 8 degrees from the specimen surface. Since these twin boundaries are at such an oblique angle to the surface, the actual width of the twin boundaries is much smaller than the apparent widths of about 700 nm and 1 μm for the lower and upper twins, respectively. The image seen on the specimen surface and the measured orientations give two possibilities for the sub-surface morphology of these boundaries. The first explanation is that there is only one twin grain that has a non-coherent ledge making it appear as two grains on the surface. The second explanation is that there simply exist two parallel twin grains. These two possibilities are shown schematically in Figure 7 with an exaggerated angle with respect to the specimen surface compared to that which exists in the grains discussed. The following discussion is applicable for either of the possible twin morphologies.

As the sample was deformed, the width of the lower twin decreased in size until it was no longer visible (as seen in Figure 5). The constrained direction of the specimen is horizontal on the images, and the elongation direction is vertical in the images shown in Figure 5. If the grains deformed according to the Taylor assumption that the strain in all grains is identical to the macroscopically imposed deformation, the width of

each of the twin grains would increase by the same percent as the height reduction. The space between the twins would correspondingly increase. A possible explanation for the observation of the twin width decreasing to zero, as suggested above, is that one twin boundary acted as a non-regenerative dislocation source, and the interface unraveled as dislocations were produced. The stress state with respect to the twin orientations, and the character of the twin boundary itself would determine whether it could act as a dislocation source, so it is not surprising that one twin could behave differently than the other.

The dislocations produced from the twin boundary would necessarily cause a curvature in lattice of the parent grain. Such information is inherent in the orientation imaging data. This curvature is best shown by creating a misorientation angle profile from a point near the position of the remaining twin boundary downwards into the grain (along the direction of highest orientation gradient). Such a plot obtained from the data after 10% deformation is shown in Figure 8. It is seen from this plot that the lattice continually rotates to about 9 degrees from the initial orientation over a distance of about 3 μm.

In a classical paper, Nye showed that the measurement of lattice curvature is directly related to the dislocation density tensor [10]. Sun, Adams and King [11] reduced Nye's work to application using data obtained during EBSD analysis. The salient features of their analysis are repeated herein, but the reader is referred to [11,12] for more complete discussion. The fundamental relation between the dislocation density tensor, $\boldsymbol{\alpha}$, and the changes in lattice orientation, $\boldsymbol{g}$, are given in component form by:

$$\alpha_{ij} = e_{ikl} g_{jl,k} \qquad (1)$$

where e_{ikl} are the components of the permutation tensor. $g_{jl,k}$ indicates the partial derivative along k of the component of the direction cosine matrix, $\boldsymbol{g}$, containing the relationship of the crystallite lattice orientation to the sample coordinate frame. Summation over repeated indices is assumed in this notation. Since $\boldsymbol{g}$ is measured along a regular grid over the surface of the specimen using orientation imaging, the $g_{jl,k}$ terms for $k = 1$ and $k = 2$ are obtained directly. No information is obtained for lattice curvature through the thickness of the specimen, so only the lattice curvature into the specimen surface is ignored and assumed to be zero in the present analysis, and our determination of the dislocation density tensor will be a lower bound estimate. Estimates of lattice curvature as a function of depth into the specimen surface could be obtained using serial sectioning techniques.

The dislocation density tensor is defined by the network of dislocations in the material at a given position. This relationship, given by Nye [10], is

$$\boldsymbol{\alpha} = \sum_s \rho^s \boldsymbol{b}^s \otimes \boldsymbol{z}^s \qquad (2)$$

where r^s is the dislocation density for a given dislocation type, s. $\boldsymbol{b}$ and $\boldsymbol{z}$ are the Burgers vector and line direction for the given type of dislocation. For FCC metals, there exist 12 screw and 24 edge types of

dislocations including <110> Burgers vectors and <110> line directions for screw dislocations, and <110> Burgers vectors and <211> line directions for edge dislocations. The solution to this series of equations is not unique with an infinite set of r^s able to satisfy the equation. In this work we adopt the lower bound approximation where the minimum dislocation density that can produce the observed curvature is assumed. It should be emphasized that the approximation of dislocation density given herein is a lower bound because the curvature into the specimen is ignored and because the minimum set of r^s that can satisfy the equations are adopted. Of course, the equations relating lattice curvature to dislocation density only consider the geometrically necessary component of the dislocation network.

As seen in Figure 8, the misorientation as a function of distance near the twin boundary under consideration is nearly linear with distance. The slope of this line is related to the $g_{jl,k}$ components necessary to determine the dislocation density. To obtain the dislocation density near the twin boundary, we considered a box of 3 x 3 μm^2 just below the remaining twin grain. Using the technique described above, a lower bound estimate for the total geometrically necessary dislocation density in this region is 2.17×10^{14} m^{-2}.

This gradient in lattice orientation did not derive entirely from any single dislocation source, such as that hypothesized to exist at the twin boundary. Obviously there are additional dislocation sources providing geometrically necessary dislocations during deformation up to 10 percent, and it is not expected that dislocations emanating from the twin boundary could account for the total dislocation content. The observations indicate that the orientation gradient near the disappearing twin grain is more severe than in surrounding locations in neighboring grains, and even in the same grain. This… The apparent width of the twin grain that disappeared is approximately 700 nm but the actual width is only about 100 nm due to the steep angle (8º) at which the boundaries intersect the specimen surface. This comprises slightly more than 3300 atomic layers of the {111} plane stretching over a distance of about 3 microns (observed width of the twin). The calculated dislocation density given above is several orders of magnitude greater than that which could be achieved by a single non-regenerative dislocation source at the twin boundary. Nevertheless, this calculation demonstrates that there is at least sufficient dislocation content to account for the observed migration of the twin boundary.

The final question to be addressed concerns that of the dislocation reaction that must be necessary to create the observed behavior. As discussed in a previous work [1], the Shockley partial 1/6 <112> dislocations must produce stair rod type dislocations to maintain slip compatibility and allow deformation to continue after the dislocations have been emitted from a boundary source. This would give the dislocation reactions the same character as that described by Foiles and Medlin [13] for the migration of annealing twin boundaries in FCC metals by thermally activated dislocation climb.

Conclusions

It has been observed in polycrystalline Cu deformed at room temperature that a fraction of the twin

boundaries in the material migrate during deformation. In a few isolated instances narrow twin grains consisting of two parallel boundaries separated by a small distance have been observed to be mechanically annihilated during this process. It is proposed that this interface migration is due to the boundaries acting as non-regenerative sources for dislocations. The orientation gradient in a parent grain near an annihilated twin was analyzed for dislocation density and it was found that sufficient geometrically necessary dislocation content was present to be consistent with the proposed mechanism.

Acknowledgments

This work was supported by the US Department of Energy, Office of Energy Efficiency and Renewable Energy, FreedomCAR and Vehicle Technologies Program Office, under DOE Idaho Operations Office Contract DE-AC07-99ID13727.

References

1. J.E. Flinn, D.P. Field, G.E. Korth, T.M. Lilo, and J. Macheret, Acta mater, 49, 2065 (2001).

2. K. Konopka, J. Mizera, and J.W. Wyrzykowski, J. Matls. Proc. Tech, 99, 255, (2000).

3. T. Nørbygaard and J.B. Bilde-Sørensen, in Proceedings of the 9th International Conference, Swansea (GB), Ed. J.D. Parker, Institute of Materials, London, p 15, 2001.

4. T. Malis and K. Tangri, Acta metall., 1979, 27, 25.

5. R.N. Singh and K. Tangri, Metall. Trans., 1970, 1, 3151.

6. K. Farrell and J.T. Houston, Scripta Metall, 5, 463 (1971).

7. Segal, V. M., Mater. Sci. Eng, A197 (1995), 157.

8. Ferrasse, S., Segal, V. M., Hartwig, K. T. and Goforth, R.M., Metall. Mater. Trans A, 28A (1997), 1047.
9. Y. Iwahashi, M. Furukawa, Z. Horita, M. Nemoto, and T.G. Langdon, Metall. Mater. Trans. A, 29A (1998), 2245.

10. S. Panchanadeeswaran, R.D. Doherty, and R. Becker, Acta mater, 44, 1233 (1996).

11. J.F. Nye, Acta metall, 1, 153 (1953).

12. S. Sun, B.L. Adams, and W.E. King, Phil. Mag A, 80, 9 (2000).

13. B.S. El-Dasher, B.L. Adams, and A.D. Rollett, Scripta Metall, 48, 145 (2003).

14. S.M. Foiles and D.L. Medlin, Mater. Sci. Eng. A319-321 (2001) 102.

Table 1 – Fraction of twin boundaries in the microstructure as a function of deformation

Percent Deformation	Fraction of Twin Boundaries
0	0.58
5	0.54
10	0.36

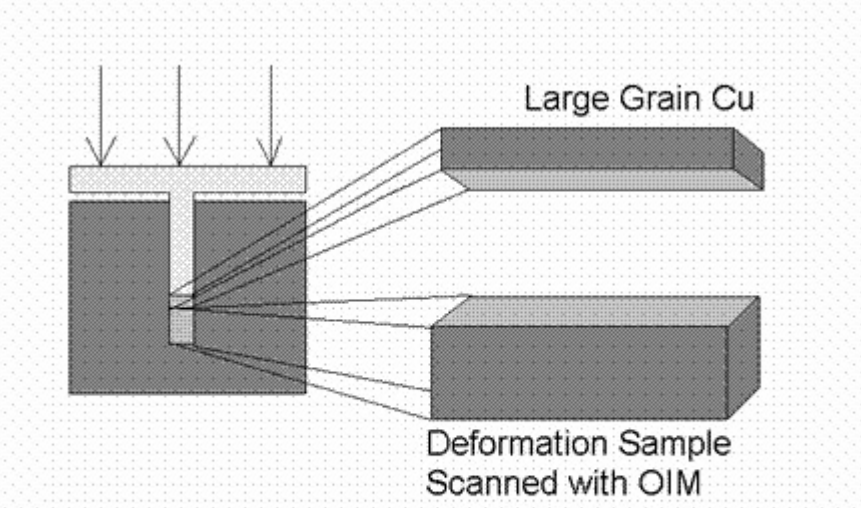

Figure 1 – Schematic of channel die deformation apparatus and specimen configuration.

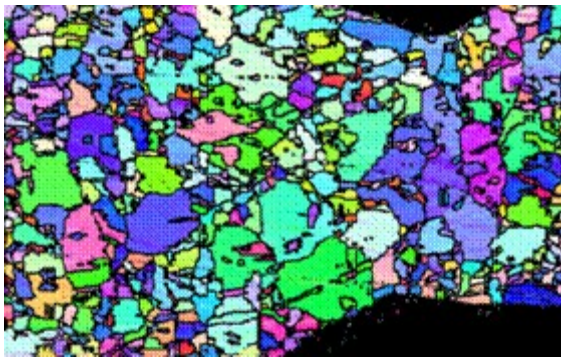

Figure 2 – Representative orientation image of the scan regions. The orientation shading key is shown at right.

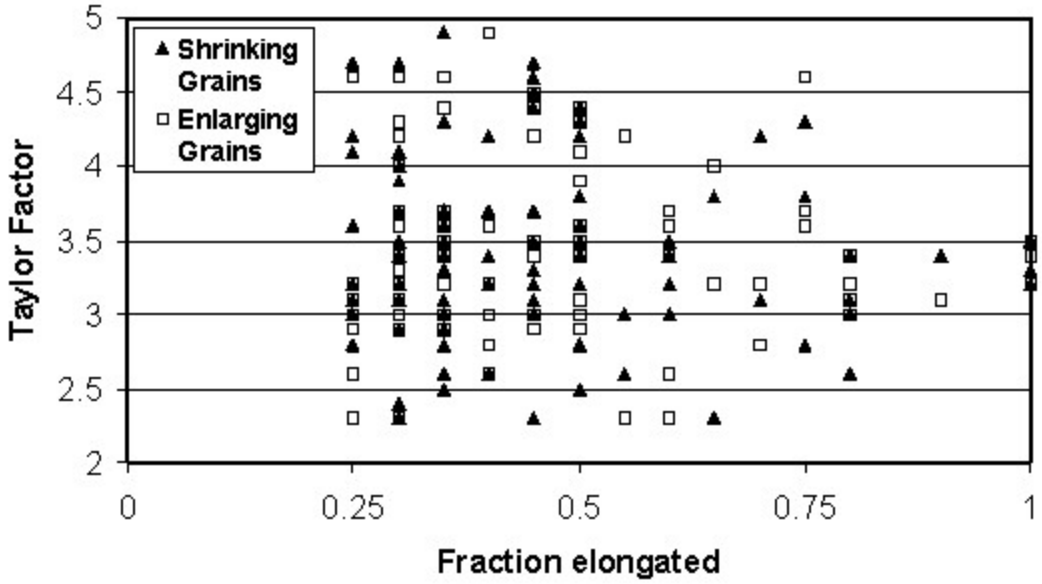

Figure 3 – Taylor factors of shrinking and enlarging grains for twin/parent grain pairs as a function of the fraction diminished in the shrinking grain.

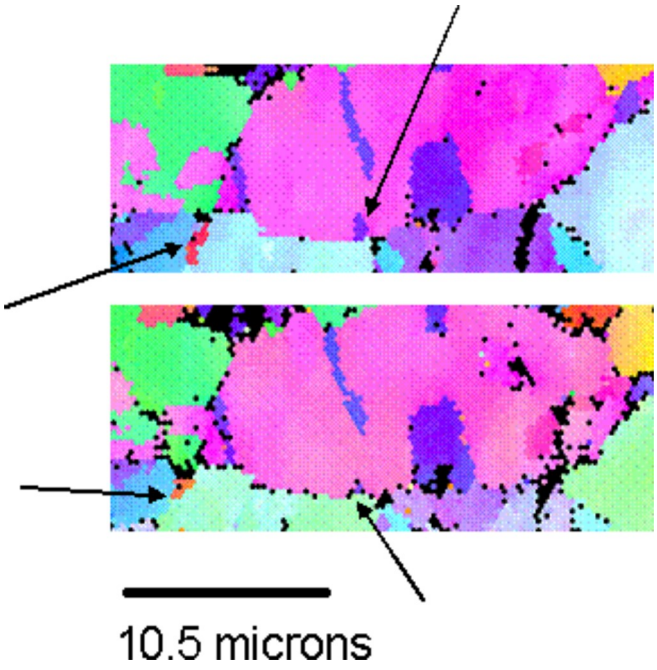

Figure 4 – Migration of incoherent twin boundaries with deformation. The top image was obtained prior to deformation and the bottom image after 10% compression. The arrows indicate the twin grains that tended to decrease in size during deformation. The orientation shading key is that shown in Figure 2.

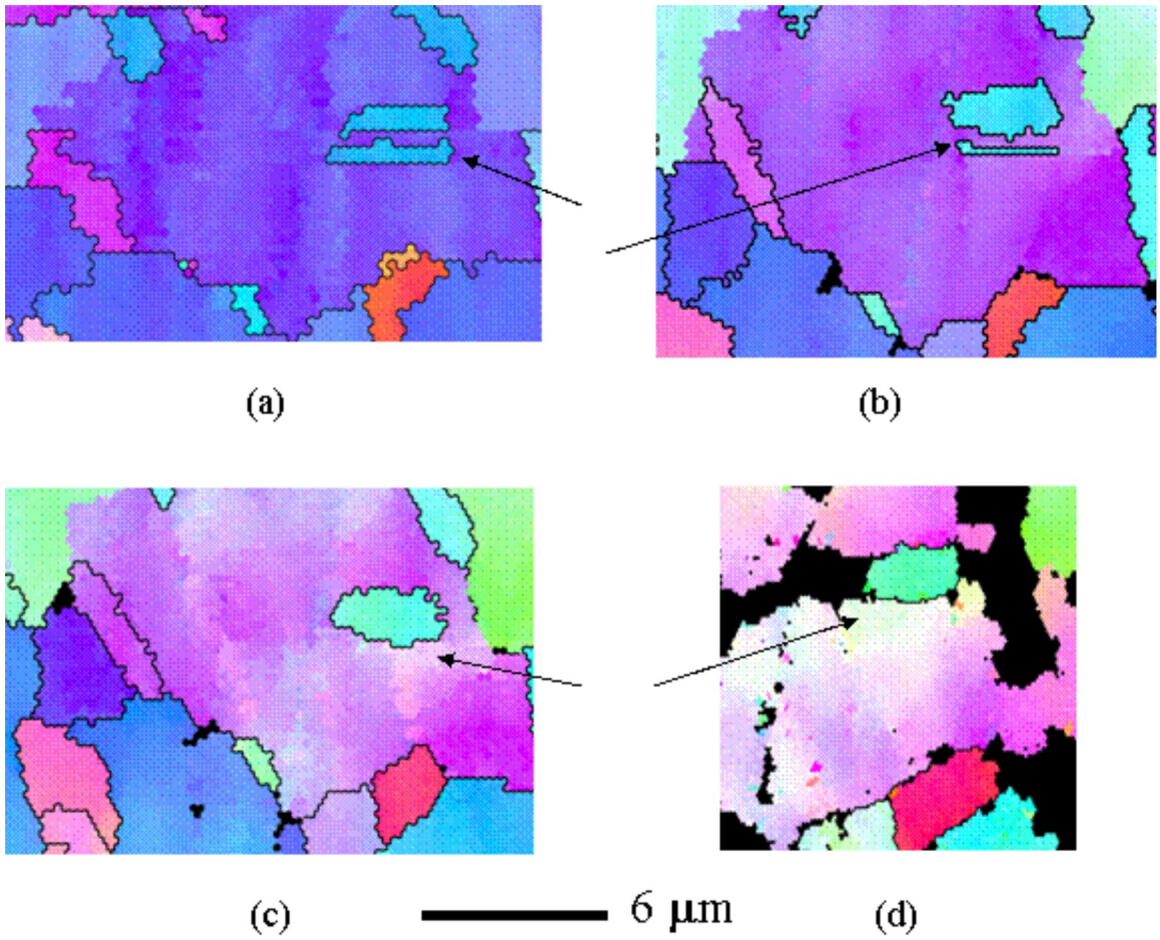

Figure 5 – Orientation images of parent and twin grains (a) before deformation, and at (b) 5%, (c) 10%, and (d) 15% deformation. Arrows indicate the location of the disappearing twin grain. The orientation shading key is that shown in Figure 2.

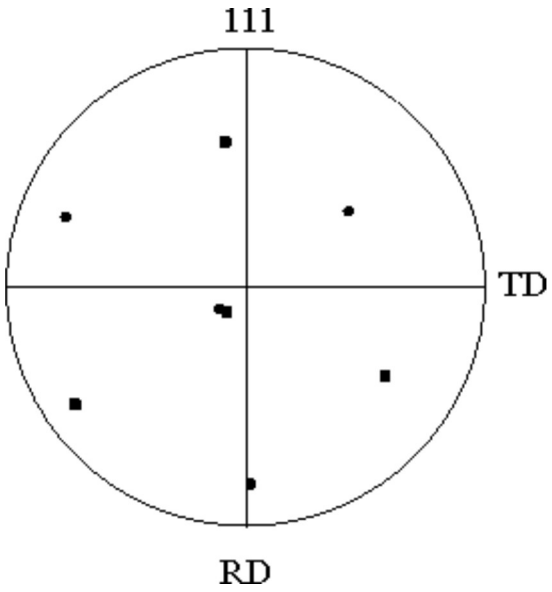

Figure 6 – {111} pole figure showing orientations of parent grain (square) and twin grains (circle) of the grains identified in Figure 3.

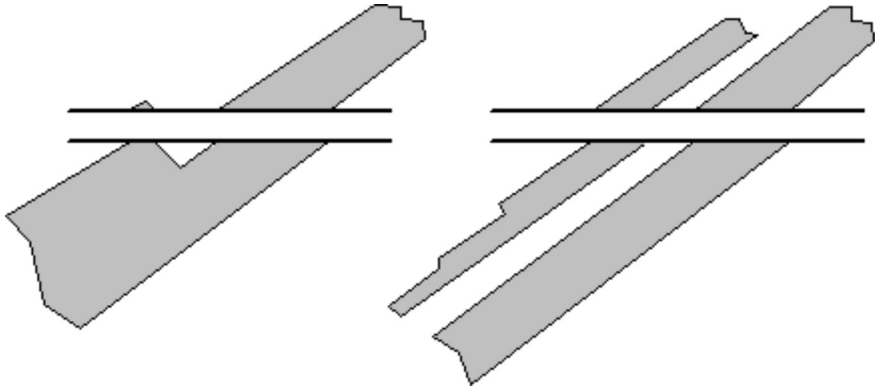

Figure 7 – Possible configurations of the twin grains as viewed from a section perpendicular to the observation plane.

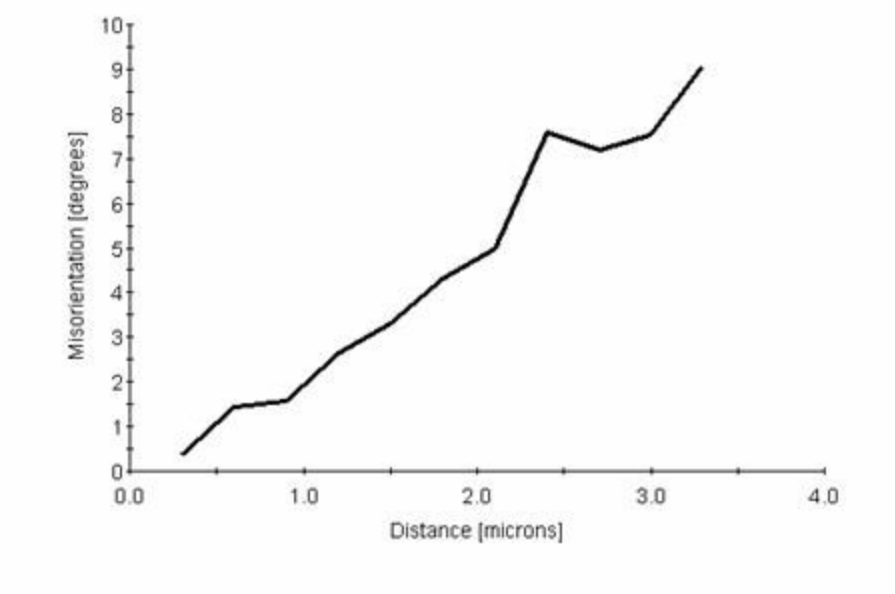

Figure 8 – Misorientation angle profile in the parent grain of the 10% deformed specimen through the region where the twin grain had disappeared.